Supercritical Fluid Extraction of *Citrus iyo* Hort. ex Tanaka Pericarp Inhibits Growth and Induces Apoptosis Through Abrogation of STAT3 Regulated Gene Products in Human Prostate Cancer Xenograft Mouse Model

Chulwon Kim, MS[1], Il Ho Lee, KMD[1], Ho Bong Hyun, MS[2], Jong-Chan Kim, PhD[3], Rajendra Gyawali, PhD[4], Seok-Geun Lee, PhD[1], Junhee Lee, KMD[1], Sung-Hoon Kim, KMD[1], Bum Sang Shim, KMD[1], Somi K. Cho, PhD[2], and Kwang Seok Ahn, PhD[1]

Abstract

Activation of signal transducer and activator of transcription 3 (STAT3) is well known to play a major role in the cell growth, survival, proliferation, metastasis, and angiogenesis of various cancer cells. Most of the citrus species offer large quantities of phytochemicals that have beneficial effects attributed to their chemical components. Our study was carried out to evaluate the anticancer effects of the pericarp of Iyokan (*Citrus iyo* Hort. ex Tanaka), locally known as yeagam in Korea, through modulation of the STAT3 signaling pathway in both tumor cells and a nude mice model. The effect of supercritical extracts of yeagam peel (SEYG) on STAT3 activation, associated protein kinases, STAT3-regulated gene products, cellular proliferation, and apoptosis was examined. The in vivo effect of SEYG on the growth of DU145 human prostate xenograft tumors in athymic *nu/nu* male mice was also investigated. We found SEYG exerted substantial inhibitory effect on STAT3 activation in human prostate cancer DU145 cells as compared to other tumor cells analyzed. SEYG inhibited proliferation and downregulated the expression of various STAT3-regulated gene products such as bcl-2, bcl-xL, survivin, IAP-1/2, cyclin D1, cyclin E, COX-2, VEGF, and MMP-9. This correlated with an increase in apoptosis as indicated by an increase in the expression of p53 and p21 proteins, the sub-G1 arrest, and caspase-3-induced PARP cleavage. When administered intraperitoneally, SEYG reduced the growth of DU145 human prostate xenograft tumors through downmodulation of STAT3 activation in athymic *nu/nu* male mice. Overall, these results suggest that SEYG extract has the potential source of STAT3 inhibitors that may have a potential in chemoprevention of human prostate cancer cells.

Keywords

[1]Kyung Hee University, Seoul, Republic of Korea
[2]Jeju National University, Jeju, Republic of Korea
[3]Korea Food Research Institute, Seongnam, Gyeonggi-do, Republic of Korea
[4]Kathmandu University, Dhulikhel, Kavre, Nepal

Corresponding Authors:
Somi Kim Cho, Faculty of Biotechnology, Jeju National University, 66 Jejudaehakno, Jeju, 690-756, Republic of Korea.
E-mail: somikim@jejunu.ac.kr
Kwang Seok Ahn, Department of Korean Pathology, College of Korean Medicine, Kyung Hee University, 1 Hoegi-Dong Dongdaemun-Gu, Seoul 130-701, Republic of Korea.
Email: ksahn@khu.ac.kr

Introduction

One potential source of signal transducer and activator of transcription 3 (STAT3) blockers is natural dietary components. A number of animal studies and epidemiological studies in human propose that fruits and vegetables can prevent cancer.[1] Citrus is a common term and genus (*Citrus*) of flowering plants in the rue family, Rutaceae. Citrus is believed to have originated from the part of Southeast Asia bordered by Northeast India, Burma (Myanmar), and the Yunnan province of China.[2] Natural and cultivated origin hybrids include commercially important fruits such as the oranges, grapefruit, lemons, some limes, and some tangerines. We describe here the bioactive potential of the fruit of *Citrus iyo* Hort. ex Tanaka (locally known as Iyokan), which is one of a variety of citrus fruits. The citrus fruits have been shown to suppress the growth of various tumors, including prostate carcinoma,[3,4] breast carcinoma,[5] colon carcinoma,[6,7] liver carcinoma,[8,9] and lung carcinoma.[10] Most of the citrus species offer large quantities of phytochemicals that have beneficial effects attributed to their chemical components: tangeretin, nobiletin, hesperetin, naringin, and naringenin. We have recently shown that nobiletin, one of citrus flavonoids, can downregulate CXC chemokine receptor type 4 and matrix metallopeptidase-9 through the suppression of the constitutive NF-κB and MAPKs activation.[11] We further observed that nobiletin can induce apoptosis and potentiate the effects of the anticancer drug 5-fluorouracil in p53-mutated SNU-16 human gastric cancer cells.[12] Moreover, tangeretin,[13] naringin,[14] naringenin,[15] and hesperetin,[16] derived from citrus fruits, are known to exhibit diverse anticancer activities in a variety of tumor cells.

The signal transducer and activator of transcription (STAT) proteins consist of a 7-member family of latent cytoplasmic transcription factors that are stimulated through tyrosine phosphorylation by various cytokines (eg, interleukin-6, tumor necrosis factor-α), growth factors (eg, epidermal growth factor, transforming growth factor-α, hepatocyte growth factor), and oncogenic kinases (eg, Src).[17] STAT activation pathways have been strongly associated with the proliferation, antiapoptosis, and chemoresistance of tumors.[18] We have previously reported that the anticancer effects of Dangyuja (*Citrus grandis* Osbeck) leaves are mediated in part through suppression of STAT3 activation.[19] It is possible that supercritical extracts of yeagam peel (SEYG) may also mediate its effects through the modulation of this pathway. Moreover, the detailed molecular mechanisms(s) by which SEYG mediates antitumor activities has not yet been fully elucidated.

Once activated, STAT3 undergoes phosphorylation-induced homodimerization, leading to nuclear translocation, DNA binding, and subsequent gene transcription. The phosphorylation is mediated through the activation of non-receptor protein tyrosine kinases called janus-like kinase (JAK). JAK1, JAK2, JAK3, and TYK2 have been implicated in the activation of STAT3.[20] In addition, the role of c-Src kinase has been demonstrated in STAT3 phosphorylation.[21] STAT3 has been shown to regulate the expression of genes that participate in oncogenesis, such as apoptosis inhibitors (bcl-xl, bcl-2, IAP-1/2, and survivin), cell-cycle regulators (COX-2, cyclin D_1, and cyclin E), and inducers of angiogenesis (MMP-9 and VEGF).[18] Thus, small molecule inhibitors of STAT3 activation have the potential for both the prevention and treatment of cancer.[22,23]

Because of the critical role of STAT3 in survival, proliferation, metastasis, and angiogenesis, we postulated that SEYG mediates its effects through the suppression of the STAT3 pathway. The results that follow indicate that SEYG specifically suppressed constitutive STAT3 activation and downregulated the expression of cell survival, proliferative, and angiogenic gene products, leading to the suppression of proliferation and the induction of apoptosis in human prostate cancer DU145 cells. SEYG also inhibited the growth of human DU145 cells and suppressed constitutive STAT3 signaling pathway in a xenograft mouse prostate model.

Materials and Methods

Plant Materials

Fruits of *Citrus iyo* Hort. ex Tanaka, locally known as yeagam, were collected from the National Institute of Subtropical Agriculture, Jeju Province, Korea. The fruits were harvested from native plants during the harvest season (from December 2011 to January 2012). Botanical samples were previously taxonomically identified, and voucher specimens were deposited in the laboratory of Dr S. K. Cho at the College of Applied Life Sciences, Jeju National University.

Supercritical Fluid Extraction

Peel of yeagam (331 g) were loaded separately into a 1-L thick-walled stainless steel thimble extraction cell and extracted at 50°C for 2 hours. The extraction was performed using CO_2 at 300 bar pressure in a diaphragm compressor (Haskel Co, Bellingham, WA). The extracts were deposited in a separator attached to a metering valve and held in a circulating bath at 0°C. Finally, the extracts were collected into a clean vial and stored at −21°C until analysis.

Reagents

An 100 mg/mL solution of SEYG was prepared in 30% ethanol (diluted in phosphate-buffered saline [PBS]), stored in

small aliquots at −20°C, diluted in the culture medium for in vitro experiments or diluted in the PBS for in vivo experiments just before use. 3-(4,5-Dimethylthiazol-2-yl)-2,5-diphenyltetrazolium bromide (MTT), propidium iodide (PI), Tris base, glycine, NaCl, sodium dodecylsulfate (SDS), and bovine serum albumin (BSA) were purchased from Sigma-Aldrich (St Louis, MO). RPMI 1640, Dulbecco's modified Eagle medium (DMEM), fetal bovine serum (FBS), and LightShift Chemiluminescent EMSA kit were obtained from Thermo Fisher Scientific Inc (Waltham, MA). 5′-Biotinylated STAT3 and Oct-1 oligonucleotide were from Bioneer Corporation (Daejeon, Korea). Alexa Fluor 488 donkey anti-rabbit IgG (H+L) antibody, 0.4% trypan blue vital stain, and antibiotic-antimycotic mixture were obtained from Life Technologies (Grand Island, NY). Anti-COX-2 antibody was obtained from BD Biosciences (San Diego, CA). Anti-phospho-JAK1, anti-JAK1, anti-phospho-JAK2, anti-JAK2, anti-phospho-Src, and anti-Src antibodies were purchased from Cell Signaling Technology (Beverly, MA). Anti-phospho-STAT3, anti-STAT3, anti-cyclin D1, anti-cyclin E, anti-p21, anti-p53, anti-bcl-2, anti-bcl-xL, anti-survivin, anti-IAP-1, anti-IAP-2, anti-VEGF, anti-MMP-9 (matrix metalloproteinase-9), anti-caspase-3, anti-cleaved caspase-3, anti-PARP, anti-Ki-67, anti-CD31, anti-β-actin, and horseradish peroxidase (HRP)–conjugated secondary antibodies were obtained from Santa Cruz Biotechnology (Santa Cruz, CA). Caspase-3 inhibitor was from Calbiochem (San Diego, CA). TUNEL (terminal transferase mediated dUTP-fluorescein nick end labeling) assay kit was from Roche Diagnostics GmbH (Mannheim, Germany). Whole-cell lysates of tumor tissues were obtained with T-PER Tissue Protein Extraction Reagent (Pierce, Rockford, IL).

Cell Lines

Human multiple myeloma U266, human myeloid leukemia K562, human prostate carcinoma DU145, PC-3, normal human prostate RWPE-1, human breast carcinoma MDA-MB-231, and human hepatocellular liver carcinoma HepG2 and mouse embryonic fibroblast (MEF) cells were obtained from the American Type Culture Collection (Manassas, VA). M2182 was kindly provided by Dr Paul B. Fisher (Virginia Commonwealth University School of Medicine, Richmond, VA). U266, K562, DU145, PC-3, M2182, RWPE-1, and MDA-MB-231 cells were cultured in RPMI 1640 medium containing 10% FBS. HepG2 and MEF cells were cultured in DMEM medium containing 10% FBS. All media were also supplemented with 100 U/mL of penicillin and 100 μg/mL of streptomycin.

MTT Assay

Cell viability was analyzed by an MTT assay to detect NADH-dependent dehydrogenase activity,[24] as described previously.[25]

Western Blotting

After the cells were treated with the indicated concentrations of SEYG, the cells were lysed and the total protein concentrations were determined by Bradford reagent (Bio-Rad, Hercules, CA). Lysates were resolved on sodium dodecyl–polyacrylamide gel electrophoresis (SDS-PAGE).[26] Western blot analysis was performed using a method described previously.[25] Statistical analysis and densitometry values for Western blot experiments were estimated by the Sigmaplot (Systat Software, Inc, San Jose, CA) and Image J software (National Institutes of Health, Bethesda, MD).

EMSA for STAT3-DNA Binding

STAT3-DNA binding was analyzed by electrophoretic mobility shift assay (EMSA) using a 5′-biotinylated STAT3 oligonucleotide (5′-GATCCTTCTGGGAATTCCTAGATC-3′ and 5′-GATCTAGGAATTCCCAGAAGGATC-3′). Oct-1 EMSA served as a loading control. The Oct-1 probe contained the sequence 5′-TTCTAGTGATTTGCATTCGACA-3′ and 5′-TGTCGAATGCAAATCACTAGAA-3′. Electrophoretic mobility shift assay (EMSA) was performed as described previously.[25] The membrane was detected following manufacturer instructions using LightShift Chemiluminescent EMSA kit (Waltham, MA).

Immunocytochemistry for STAT3 Localization

Immunocytochemistry was performed as described previously.[27]

Monitoring of Cell Growth With the RTCA MP Instrument

Cell growth behavior was continuously monitored for 48 hours using the xCELLigence RTCA MP Instrument (Roche Diagnostics GmbH, Mannheim, Germany). Background impedance was measured in 100 μL cell culture medium per well. The final volume was adjusted to 200 μL cell culture medium, including 5×10^3 cells/well. After plating, impedance was recorded in 15-minute intervals. All experiments were performed in triplicates. Cell Index (CI) values were normalized to the time point of 200 μg/mL of SEYG administration (referred to as normalized CI).

Transfection of Plasmids

We investigated the ability of commercially available electroporation systems, the Neon Transfection System (Invitrogen, Carlsbad, CA). Transfection efficiency was measured by Western blot analysis. MEF cells were prepared for transfection after cells were resuspended with 120 μL of Neon Resuspension Buffer R for every 1 million cells.

For electroporation, MEF cells with 1 μg of pMXs-STAT3C or pMXs-gw plasmids were aliquoted into a sterile microcentrifuge tube. A Neon Tip was inserted into the Neon Pipette and the mixture was aspirated into the tip avoiding air bubbles. The Neon Pipette was then inserted into the Neon Tube containing 3 mL of Neon Electrolytic Buffer E in the Neon Pipette Station. MEF cells were pulsed once with a voltage of 1350 and a width of 30. After 48 hours of transfection, MEF cells were treated with 200 μg/mL of SEYG for 6 hours or 24 hours. Then whole-cell extracts were prepared for phospho-STAT3 (Tyr705), STAT3, PARP, cyclin D1, and β-actin analysis by Western blotting.

Cell Cycle Analysis

Cell cycle analysis was performed as described previously.[28]

Annexin V Assay

One of the early indicators of apoptosis is the rapid translocation and accumulation of the membrane phospholipid phosphatidylserine from the cell's cytoplasmic interface to the extracellular surface. This loss of membrane asymmetry can be detected using the binding properties of annexin V. To detect apoptosis, we used annexin V antibody conjugated with the fluorescent dye fluorescein isothiocyanate (FITC). Annexin V assay was performed using a method described previously.[28]

Studies With Caspase-3 Inhibitor

DU145 cells were plated at a density of 1×10^6 cells/well in a 60-mm plate. The cells were pretreated with 20 μM of caspase-3 inhibitor for 2 hours and then treated with SEYG for an additional 24 hours, and then subjected to annexin V and PI staining. The cells were washed and observed accordingly with flow cytometry (Becton-Dickinson, Heidelberg, Germany). Acquisition and analysis of the data were performed using Cell Quest 3.0 software.

TUNEL Assay

TUNEL assay was performed as described previously.[29]

Animals

All procedures involving animals were reviewed and approved by KHU Institutional Animal Care and Use Committee (KHUASP(SE)-13-025). Six-week-old athymic *nu/nu* male mice (NARA Biotech, Seoul, Korea) were implanted subcutaneously in the right flank with DU145 cells. The animals were housed (11 mice/cage) in the standard mice plexiglass cages in a room maintained at constant temperature and humidity under 12-hour light and dark cycle and fed with regular autoclaved mouse chow with water ad libitum. None of the mice exhibited any lesions and all were tested pathogen-free. Before initiating the experiment, we acclimatized all mice to a pulverized diet for 3 days.

Subcutaneous Implantation of DU145 Cells

DU145 cells were harvested from subconfluent cultures, washed once in serum-free medium, and resuspended in PBS. Only suspensions consisting of single cells, with >90% viability, were used for the injections. DU145 cells (4×10^6/100 μL PBS-Matrigel [1:1]) were injected subcutaneously into the right flank of the mice. To prevent leakage, a cotton swab was held cautiously for 1 minute over the site of injection.

Experimental Protocol

When tumors have reached 0.25 cm in diameter, the mice were randomized into the following treatment groups (n = 11 per group). Group I was given PBS (200 μL, intraperitoneally [ip] thrice/week), group II was given SEYG (50 mg/kg body weight, ip thrice/week), and group III was given SEYG (200 mg/kg body weight, ip thrice/week). Therapy was continued for 4 weeks, and the animals were euthanized 1 week later. Primary tumors were excised and the final tumor volume was measured as $V = 4/3\pi r^3$, where r is the mean radius of the 3 dimensions (length, width, and depth). Half of the tumor tissue was fixed in formalin and embedded in paraffin for immunohistochemistry and routine hematoxylin and eosin (H&E) staining. The other half was snap frozen in liquid nitrogen and stored at −80°C.

Western Blot Analysis for Tumor Tissues

Prostate tumor tissues (75-100 mg) from control and experimental mice were minced and incubated on ice for 30 minutes in 0.5 mL of ice-cold T-PER Tissue Protein Extraction Reagent (Pierce, Rockford, IL). The minced tissue was centrifuged at $16\,000 \times g$ at 4°C for 20 minutes. The proteins were then fractionated by SDS-PAGE, electrotransferred to nitrocellulose membranes, blotted with each antibody, and detected by enhanced chemiluminescence (ECL) kit (GE Healthcare, Waukesha, WI). Densitometry values for Western blot experiments were estimated by the Image J software (National Institutes of Health, Bethesda, MD).

Immunohistochemical Analysis of Prostate Tumor Samples

Solid tumors from control and various treatment groups were fixed with 10% phosphate-buffered formalin, processed, and embedded in paraffin. Sections were cut and deparaffinized in

xylene, and dehydrated in graded alcohol and finally hydrated in water. Antigen retrieval was performed by boiling the slide in 10 mM sodium citrate (pH 6.0) for 30 minutes. Immunohistochemistry was performed following manufacturer instructions (ImmPRESS Reagent Kit; Vector Laboratories, Burlingame, CA). Briefly, endogenous peroxidases were quenched with 3% hydrogen peroxide. Nonspecific binding was blocked by incubation in the blocking reagent in the ImmPRESS Reagent Kit according to the manufacturer's instructions. Sections were incubated overnight with primary antibodies as follows: anti-Ki-67, anti-CD31, anti-cleaved caspase-3 (each at 1:100 dilutions). Slides were subsequently washed several times in PBS and were incubated with ImmPRESS reagent according to the manufacturer's instructions. Immunoreactive species were detected using 3,3-diaminobenzidine tetrahydrochloride (DAB) as a substrate. Sections were counterstained with Gill's hematoxylin and mounted under glass cover slips. Images were taken using an Olympus BX51 microscope (magnification, 20×). Positive cells (brown) were quantitated using the Image-Pro plus 6.0 software package (Media Cybernetics, Inc, Rockville, MD).

Gas Chromatography–Mass Spectrometry (GC-MS) Analysis

Chromatographic analysis was carried out using a Shimadzu GC-MS (model QP-2010, Shimadzu Co, Kyoto, Japan) attached to AOC-5000 autosampler in electron impact mode. The ionization voltage was 70 eV, and the temperatures of the injector and interface were 250°C and 290°C, respectively. The capillary column used was an Rtx-5MS (30 m length, 0.25 mm internal diameter, and 0.25 μm film thickness). The oven temperature was programmed at 60°C (isothermal for 2 minutes) and was ramped to 250°C at 5°C/min and to 310°C at 8°C/min (isothermal for 12 minutes). Helium was used as the carrier gas at a flow rate of 1 mL/min with 57.4 kPa pressure, and an injector volume of 1 μL using a 1:10 split ratio. Mass range was from m/z 40 to 500 amu. The extracts of the fruits were solubilized in n-hexane, filtered through a 0.20-μm syringe filter (Advantec, Tokyo, Japan), and aliquots were injected into the GC-MS. Mass spectra of each compound were tentatively identified with the mass spectral data contained within the WILEY7 and NIST05 libraries and by their Kovats indices relative to C_7-C_{30} n-alkanes (Sigma-Aldrich, St Louis, MO) on an Rtx-5MS column. Further tentative identification was completed by comparing the mass spectra with those of authentic standards.[30]

For the determination of concentration of major compounds, limonene, linalool, and geranyl acetate in extract, calibration curves of reference standards at 3 concentrations were prepared in chloroform: 0.5, 1, and 2 μg/mL for limonene, 0.25, 0.5, and 1 μg/mL for linalool, and 0.05, 0.1, and 0.2 μg/mL for geranyl acetate, respectively, in the same condition.

Statistical Analysis

Statistical analysis was performed by Student's t test and one-way analysis of variance, (ANOVA). A P value of less than .05 was considered statistically significant.

Results

SEYG Exerts Cytotoxicity Against Various Types of Human Cancer Cells

To determine cytotoxicity, cultured human multiple myeloma (U266), human myeloid leukemia (K562), human prostate carcinoma (DU145), human breast carcinoma (MDA-MB-231), human hepatocellular liver carcinoma (HepG2), and normal human prostate (RWPE-1) cells were treated with indicated concentrations of SEYG for 24 hours, and viability was measured by MTT assay. As shown in Figure 1A, SEYG broadly inhibited the viability of 5 tumor cells in a dose-dependent manner. The results indicate that inhibition of cell viability by SEYG is cell type nonspecific. However, SEYG had no substantial effect on the suppression of cell viability in RWPE-1 cells.

SEYG Inhibits Constitutive STAT3 Phosphorylation in Human Prostate Cancer DU145 Cells

Previous studies have shown that STAT3 is a key point of convergence of multiple oncogenic signaling pathways. We next investigated whether SEYG can modulate constitutive STAT3 activation in 5 tumor cells. Because U266, K562, DU145, MDA-MB-231, and HepG2 cells have been shown to express constitutive STAT3 activation,[25,31,32] we set out to determine whether SEYG could inhibit STAT3 phosphorylation in these cells. As shown in Figure 1B, the constitutive activation of STAT3 was clearly suppressed by SEYG in DU145 cells. However, SEYG had a minimal effect on U266, MDA-MB-231, and HepG2 cells. In addition, SEYG had no effect on the suppression of constitutive STAT3 phosphorylation in K562 cells. Furthermore, as shown in Figure 1C, we determined whether SEYG could suppress STAT3 phosphorylation in various prostate cancer cell lines. We found that SEYG suppressed the constitutive phosphorylation of STAT3 in DU145, PC-3, and M2182 prostate cancer cells.

SEYG Suppresses Constitutive STAT3 Phosphorylation in a Time- and Dose-Dependent Manner

Human prostate cancer (DU145) cells are well known to express constitutively active STAT3.[25] Whether SEYG can modulate the constitutive STAT3 activation in the cells was
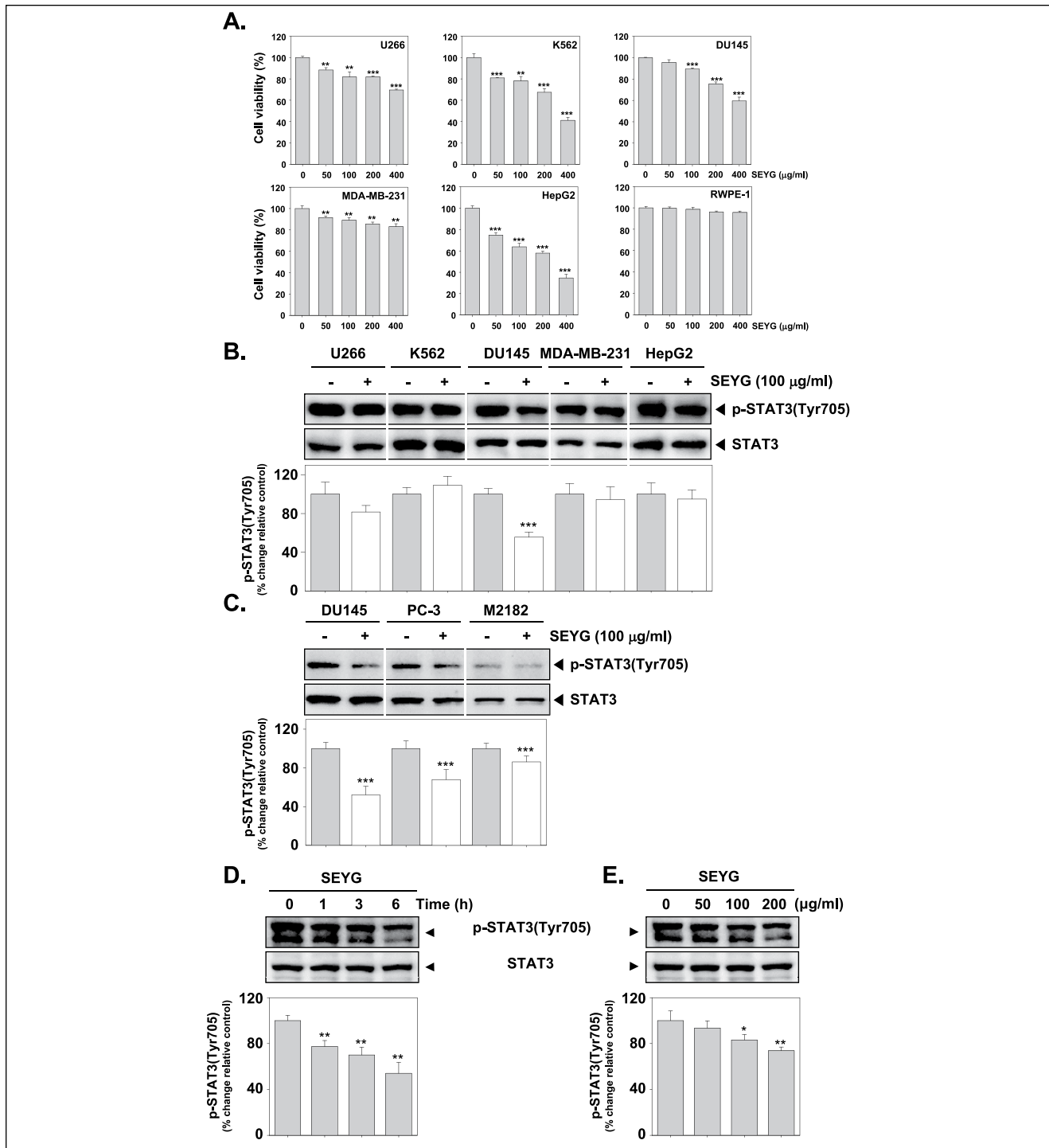
Figure 1. SEYG suppresses p-STAT3 levels in a time- and dose-dependent manner. (A) U266, K562, DU145, MDA-MB-231, HepG2, and RWPE-1 cells (1×10^4 cells/well) were incubated at 37°C with various indicated concentrations of SEYG for 24 hours, and the viable cells were assayed using the MTT reagent. ***P < .001 compared to nontreated. (B and C) Cells (1×10^6 cells/well) were incubated with the indicated concentrations of SEYG for 6 hours. Whole-cell extracts were prepared, then equal amounts of lysates were analyzed by Western blot analysis using antibodies against p-STAT3 and STAT3. The results shown here are representative of 3 independent experiments. Graphs represent band intensities of indicated proteins. All data were expressed as mean ± SD. ***P < .001 versus control. (D and E) DU145 cells (1×10^6 cells/well) were treated with various indicated concentrations of SEYG and time intervals. Then equal amounts of lysates were analyzed by Western blot analysis using antibodies against p-STAT3 (Tyr705) and STAT3. The results shown here are representative of 3 independent experiments. Graphs represent band intensities of indicated proteins. All data were expressed as mean ± SD. **P < .01 versus control.

investigated. We determined the incubation time with SEYG required for the suppression of STAT3 activation in DU145 cells. As shown in Figure 1D (*upper panel*), the inhibition was time-dependent, with strong inhibition occurring at around 6 hours, with no effect on the expression of STAT3 (Figure 1D, *lower panel*). As shown in Figure 1E (*upper panel*), SEYG suppressed the constitutive activation of STAT3 in a concentration-dependent manner, with substantial inhibition occurring at 200 μg/mL. SEYG had no effect on the expression of STAT3 protein (Figure 1E, *lower panel*).

SEYG Suppresses Constitutive Activation of JAK1/JAK2

STAT3 has been reported to be activated by the soluble tyrosine kinases of the Janus family (JAK).[20] Because JAK1/JAK2 are the main kinases involved, we examined the effect of SEYG on JAK1/JAK2 activation. As shown in Figure 2A-D, both JAK1 and JAK2 were constitutively active in DU145 cells and the treatment with SEYG clearly suppressed this phosphorylation in a time- and concentration-dependent manner.

SEYG Inhibits Constitutive Activation of Src

Because STAT3 is also activated by soluble tyrosine kinases of the Src kinase families,[21] we determined the effect of SEYG on the constitutive activation of Src kinase in DU145 cells. We found that SEYG suppressed the constitutive phosphorylation of Src kinase (Figure 2E and F, *upper panel*). The levels of total Src kinase remained unchanged under the same conditions (Figure 2E and F, *lower panel*). Overall, our data clearly indicate that SEYG may block the cooperation of JAK1/2 and Src involved in tyrosyl phosphorylation of STAT3.

SEYG Inhibits Binding of STAT3 to the DNA

Because tyrosine phosphorylation causes the dimerization of STATs and their translocation to the nucleus, where they bind to DNA and regulate gene transcription,[33] we determined whether SEYG suppresses the DNA binding activities of STAT3. EMSA analysis of nuclear extracts prepared from DU145 cells showed that SEYG reduced STAT3-DNA binding activities in a dose-dependent manner (Figure 3A). These results show that SEYG abrogates the DNA binding ability of STAT3.

SEYG Reduces Nuclear Pool of STAT3 in Tumor Cells

Because the active dimer of STAT3 is capable of translocating to the nucleus and inducing transcription of specific target genes,[33] we determined whether SEYG suppresses the nuclear translocation of STAT3. Immunocytochemistry results (Figure 3B) clearly demonstrate that SEYG reduced the translocation of STAT3 into the nucleus in DU145 cells.

SEYG Suppresses Cell Proliferation in Human Prostate Cancer Cells

To specifically examine the antitumor activity of SEYG on DU145 cells, the cells were treated with 200 μg/mL concentrations of SEYG, and then cell viability was analyzed using every 15-minute time intervals with the xCELLigence RTCA MP Instrument (Roche Diagnostics GmbH). As shown in Figure 3C, SEYG significantly suppressed cell proliferation in prostate cancer cells in a time-dependent manner.

SEYG Downregulates Expression of Various Proteins Involved in Antiapoptosis, Proliferation, and Angiogenesis

Because bcl-2, bcl-xL, survivin, IAP-1, and IAP-2 have been implicated in apoptosis and mitochondrial dysfunction, we next examined the effects of SEYG on the constitutive expression of these proteins. We found that SEYG suppressed the expression of antiapoptotic gene products in a dose-dependent manner (Figure 3D). Also, SEYG repressed proteins linked with cell proliferation (cyclin D1, cyclin E, and COX-2) and angiogenesis (MMP-9 and VEGF; Figure 3E and F).

SEYG Induces the Expression of Both p53 and p21

p53 is important in multicellular organisms, where it regulates the cell cycle and, thus, functions as a tumor suppressor that is involved in preventing development of cancer.[34] The expression of p21 is controlled by the tumor suppressor protein p53.[35] The cyclin-dependent kinase inhibitor p21 is a prototypical member of the Cip/Kip family of cyclin-dependent kinase inhibitors. It negatively modulates cell cycle progression by inhibiting the activities of cyclin E/CDK2 and cyclin D/CDK4 complexes and blocks DNA replication by binding to proliferating cell nuclear antigen.[36] We found that SEYG induced the expression of both p53 and p21 in a concentration-dependent manner in prostate tumor cells (Figure 4A).

SEYG Activates Caspase-3 and Causes PARP Cleavage

Cells were treated with indicated concentration of SEYG for 24 hours and then examined for caspase activation by Western blot using specific antibodies. We found a dose-dependent
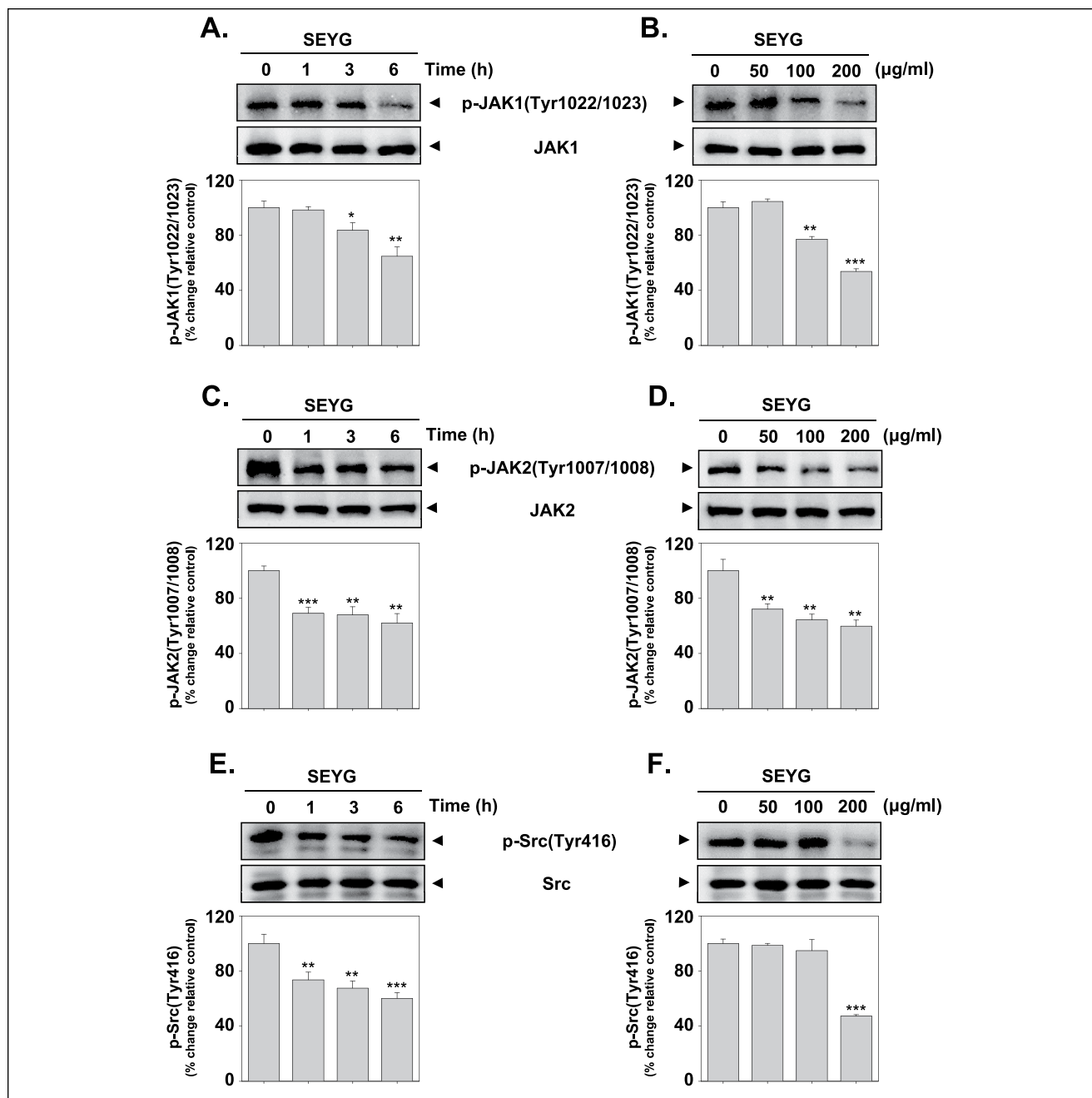
Figure 2. SEYG downregulates p-JAK1, JAK2, and Src levels in a time- and dose-dependent manner. (A-F) DU145 cells (1 × 10^6 cells/ well) were treated with various indicated concentrations of SEYG and time intervals. Then equal amounts of lysates were analyzed by Western blot analysis using antibodies against p-JAK1 (Tyr1022/1023), JAK1, p-JAK2 (Tyr1007/1008), JAK2, p-Src (Tyr416), and Src. The results shown here are representative of 3 independent experiments. Graphs represent band intensities of indicated proteins. All data were expressed as mean ± SD. **P < .01 versus control.

activation of caspase-3 by SEYG (Figure 4B, *first panel*). Activation of downstream caspases led to the cleavage of a 116 kDa PARP protein into 87 kDa fragments (Figure 4B, *Second panel*). Taken together, these results suggest that SEYG induces caspase-3-dependent apoptosis in DU145 cells.

Overexpression of STAT3 Attenuates SEYG-Mediated Apoptosis

We investigated whether overexpression of STAT3 by pMXs-STAT3C plasmid can prevent the effects of SEYG. The cells transfected with pMXs-STAT3C clearly showed
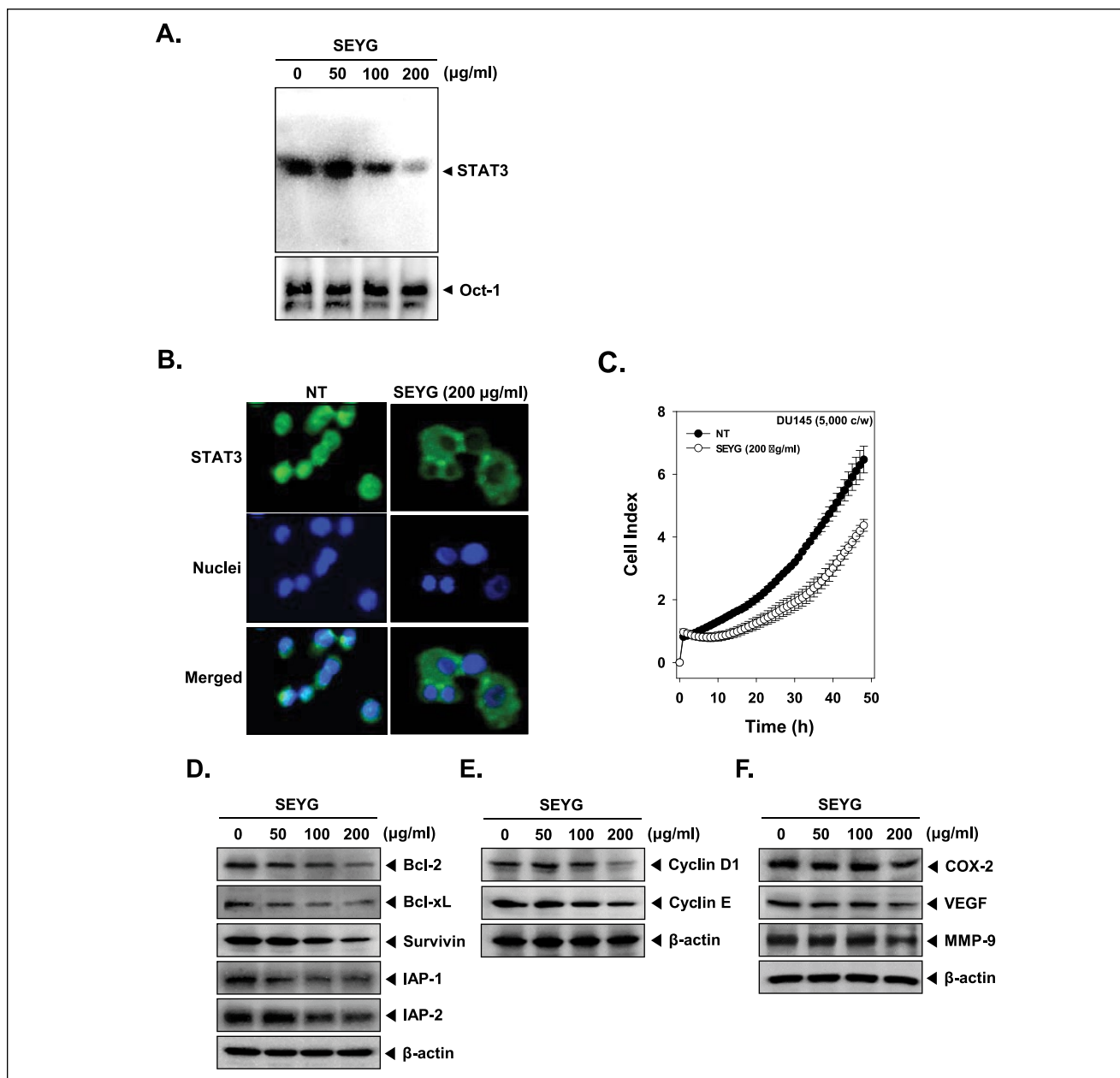
Figure 3. SEYG inhibits binding of STAT3 to the DNA and expression of various gene products in human prostate cancer cells. (A) SEYG suppresses STAT3 binding activity. DU145 cells (1 × 10^6 cells/well) were treated with various indicated concentrations of SEYG for 6 hours, analyzed for nuclear STAT3 levels by EMSA. Oct-1 EMSA is shown as a loading control. (B) SEYG causes the inhibition of translocation of STAT3 to the nucleus. After 6 hours of SEYG treatment, the cells were fixed and permeabilized. STAT3 (green) was immunostained with rabbit anti-STAT3 followed by FITC-conjugated secondary antibodies and the nuclei (blue) were stained with DAPI. The third panels show the merged images of the first and second panels. The results shown are representative of 2 independent experiments. (C) Cell proliferation assay was performed using the Roche xCELLigence Real-Time Cell Analyzer (RTCA) DP instrument (Roche Diagnostics GmbH) as described in "Material and Methods." After DU145 cells (5 × 10^3 cells/well) were seeded onto 96-well E-plates and continuously monitored using impedance technology. (D-F) DU145 cells (1 × 10^6 cells/well) were incubated with the indicated concentrations of SEYG for 24 hours. Whole-cell extracts were prepared, and 20 μg of the whole-cell lysate was resolved by SDS-PAGE, electrotransferred to nitrocellulose membrane, sliced from the membrane based on the molecular weight, and then probed with antibodies against bcl-2, bcl-xL, survivin, IAP1/2, cyclin D1, cyclin E, COX-2, VEGF, and MMP-9 as described in "Materials and Methods." The same blots were stripped and reprobed with β-actin antibody to verify equal protein loading. The results shown here are representative of 3 independent experiments.

Figure 4. SEYG induces apoptosis by PARP cleavage through activation of caspase-3. (A) DU145 cells (1×10^6 cells/well) were incubated with the indicated concentrations of SEYG for 24 hours. Whole-cell extracts were prepared, and 20 μg of the whole-cell lysate was resolved by SDS-PAGE, electrotransferred to nitrocellulose membrane, sliced from the membrane based on the molecular weight, and then probed with antibodies against p53 and p21 as described in "Materials and Methods." The same blots were stripped and reprobed with β-actin antibody to verify equal protein loading. The results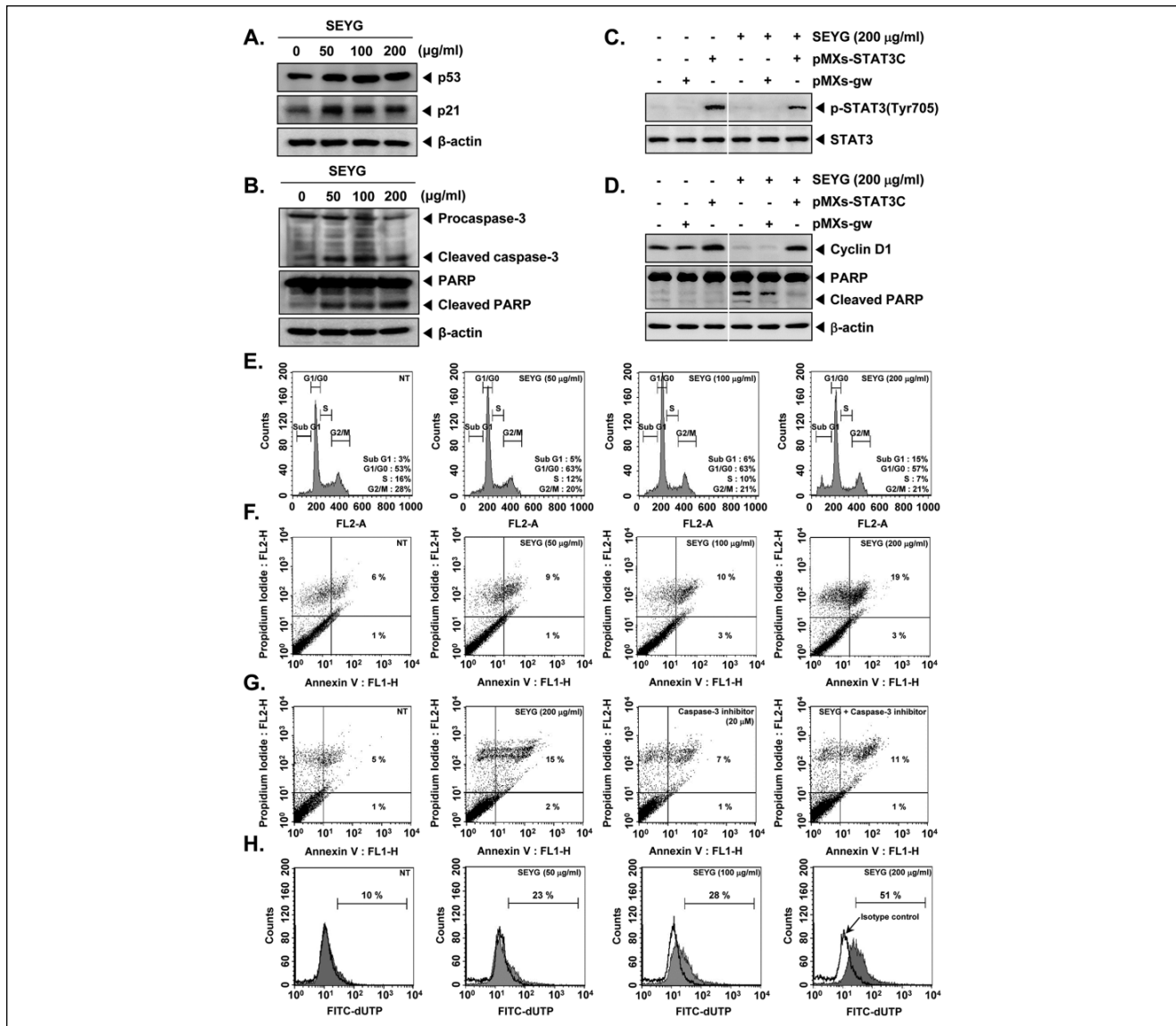 shown here are representative of 3 independent experiments. (B) After DU145 cells (1×10^6 cells/well) were seeded onto 6-well plates, they were treated with various indicated concentrations of SEYG for 24 hours. Thereafter, equal amounts of lysates were analyzed by Western blot analysis using antibodies against caspase-3 and PARP. The same blots were stripped and reprobed with β-actin antibody to verify equal protein loading. (C) MEF cells were transiently transfected with pMXs-STAT3C or pMXs-gw (control vector) plasmid. STAT3C protein was overexpressed in pMXs-STAT3C tranfected MEF cells compared to control. Transiently transfected cells were treated with indicated concentrations of SEYG for 6 hours. Then, equal amounts of lysate were analyzed by Western blot analysis using antibodies against phospho-STAT3 (Tyr705) and STAT3. (D) MEF cells were transiently transfected with pMXs-STAT3C or pMXs-gw (control vector) plasmid. STAT3C protein was overexpressed in pMXs-STAT3C tranfected MEF cells compared to control. Transiently transfected cells were treated with indicated concentrations of SEYG for 24 hours. Equal amounts of lysate were analyzed by Western blot analysis using antibody against cyclin D1 and PARP. The same blots were stripped and reprobed with β-actin antibody to verify equal protein loading. The results shown here are representative of 3 independent experiments. (E) After DU145 cells (1×10^6 cells/well) were seeded onto 6-well plates, they were incubated with the indicated concentrations of SEYG for 24 hours. Then, the cells were fixed and analyzed using flow cytometry. The results shown here are representative of 3 independent experiments. (F) Cells were treated with indicated concentrations of SEYG for 24 hours. Thereafter, they were incubated with anti-annexin V antibody conjugated with FITC plus PI and analyzed with a flow cytometer for apoptotic effects. The results shown here are representative of 3 independent experiments. (G) Cells were treated with indicated concentrations of SEYG and caspase-3 inhibitor for 24 hours. Thereafter, they were incubated with anti-annexin V antibody conjugated with FITC plus PI and analyzed with a flow cytometer for apoptotic effects. The results shown here are representative of 3 independent experiments. (H) Cells were treated with indicated concentrations of SEYG for 24 hours. Cells were fixed, stained with TUNEL assay reagent, and then analyzed with a flow cytometer.

overexpression of phospho-STAT3 (Tyr705) as compared with those transfected with only control plasmid, and the overexpression of STAT3 was clearly inhibited by SEYG treatment in MEF cells (Figure 4C). As shown in Figure 4D, overexpression of STAT3 led to the attenuation of SEYG-mediated suppression of cyclin D1 and cleavage of PARP as compared to the control, indicating that STAT3 is one of the major molecular targets involved in SEYG-induced apoptosis.

SEYG Causes the Accumulation of the Cells in the Sub-G1 Phase of the Cell Cycle

We set out to determine the effect of SEYG on cell cycle phase distribution. After treatment for 24 hours, SEYG induced an increased accumulation of 15% of the cell population in the sub-G1 phase, which is indicative of apoptosis (Figure 4E).

SEYG Induces Substantial Apoptosis

We also examined the apoptosis-inducing effects of SEYG by using the annexin V assay, which detects phosphatidylserine externalization (Figure 4F). When we further examined for late apoptosis by analyzing DNA strand breaks using the TUNEL assay, apoptotic cells were also significantly increased on SEYG treatment as observed by flow cytometric analysis (Figure 4H).

Specific Blockade of Caspase-3 Activation Abrogates SEYG-Induced Apoptosis

To determine whether a specific caspase-3 inhibitor blocks SEYG-induced apoptosis in DU145 cells, annexin V assay was performed. We found that the SEYG-induced apoptosis was suppressed by the caspase-3 inhibitor, indicating the significance of caspase-3 activation for SEYG-induced apoptosis in DU145 cells (Figure 4G).

SEYG Induces Antitumor Effects in a Xenograft Prostate Tumor Model in Nude Mice

We examined the therapeutic potential of SEYG on the growth of subcutaneously implanted human prostate cancer cells in nude mice. The experimental protocol is depicted in Figure 5A. DU145 cells were implanted subcutaneously in the right flank of nude mice. When tumors had reached 0.25 cm in diameter after a week, the mice were randomized into 3 groups and we started the treatment as per the experimental protocol. The tumor diameters were measured at 5-day intervals. The treatment was continued for 4 weeks and animals were sacrificed after 5 weeks. The tumors were excised and the tumor diameters were measured. We found that the tumor volume increased rapidly in the control group compared with the other treatment groups (Figure 5B). We found that SEYG when given at 200 mg/kg body weight considerably inhibited the growth of the tumor at day 25 after treatment ($P < .01$ when compared to control; Figure 5C and D). Furthermore, the lowest mean tumor weight was found with SEYG when given at 200 mg/kg body weight (Figure 5E).

SEYG Inhibits Ki-67 and CD31 Expression and Increases Levels of Cleaved Form of Caspase-3 Expression

While Ki-67-positive index is used as a marker for cell proliferation, the CD31 index is a marker for microvessel density. Whether SEYG modulate these markers was examined. Figure 6A shows that SEYG significantly downregulated the expression of Ki-67 in prostate cancer DU145 tissue (***$P < .001$ vs vehicle). Similarly, when examined for CD31, we found that SEYG significantly reduced the CD31 expression as compared to control group (Figure 6B; **$P < .01$ vs vehicle). Cleaved form of caspase-3 was significantly increased in the SEYG-treated group as compared with the control group (Figure 6C; ***$P < .001$ vs vehicle).

SEYG Inhibits Phosphorylation of STAT3, JAK1, JAK2, and Src in Prostate Tumor Tissues

We also evaluated the effect of SEYG on phosphorylation level of STAT3, JAK1, JAK2, and Src in prostate tumor tissues. Figure 6D shows that SEYG was substantially effective in suppressing the expression of p-STAT3, p-JAK1, p-JAK2, and p-Src at 200 mg/kg. SEYG had no effect on the expression of STAT3, JAK1, JAK2, and Src proteins in tumor tissues.

SEYG Downregulates Expression of Various Proteins Involved in Antiapoptosis, Proliferation, and Angiogenesis in Prostate Tumor Tissues

We next examined whether SEYG can modulate the constitutive expression of antiapoptotic proteins in tumor tissues, as examined by Western blot analysis. We found that SEYG suppressed the expression of bcl-2, bcl-xL, survivin, IAP-1, and IAP-2 in a dose-dependent manner (Figure 6E). Also, SEYG repressed proteins linked with cell proliferation (COX-2, cyclin D1, cyclin E, and MMP-9) and angiogenesis (COX-2, MMP-9, and VEGF; Figure 6F).

SEYG Induces the Expression of Both p53 and p21 in Tumor Tissues

To determine whether SEYG induces expression of p53 and p21, we examined the expression of these proteins in
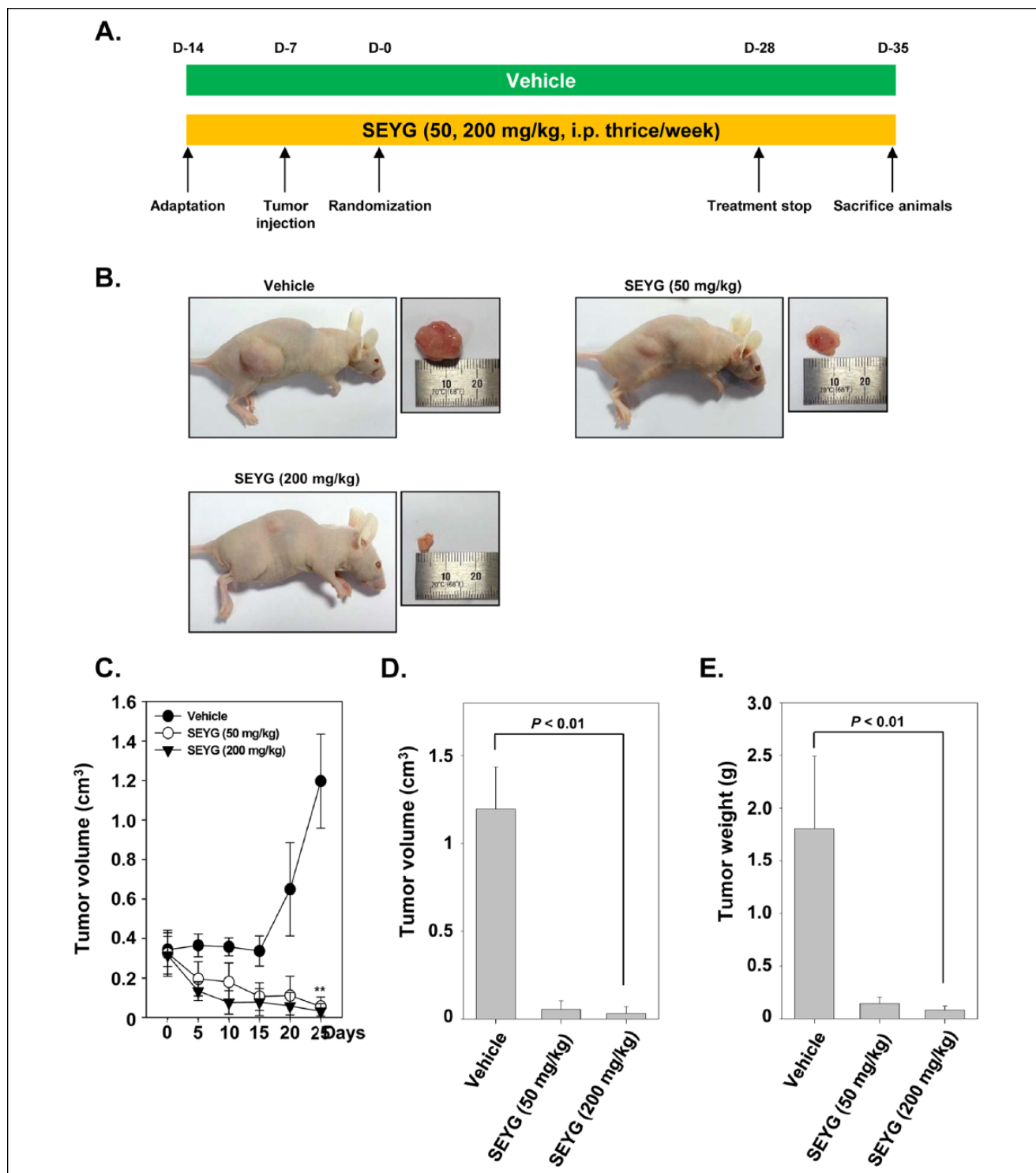
Figure 5. Effects of SEYG in human prostate cancer cells growth in nude mice induced by DU145. (A) Schematic representation of experimental protocol described in "Materials and Methods." DU145 cells (4×10^6 cells/mice) were injected subcutaneously into the right flank of the mice. The animals were randomized after 1 week of tumor cell injection into 3 groups based on tumor volume. Group I was given PBS (200 μL, ip thrice/week), group II was given SEYG (50 mg/kg body weight, ip thrice/week), and group III was given SEYG (200 mg/kg body weight, ip thrice/week). (B) Necropsy photographs of mice bearing subcutaneously implanted prostate tumors. (C) Tumor volumes in mice measured during the course of experiment and calculated using the formula $V = 4/3\pi r^3$, ** indicates $P < .01$. (D) Tumor volumes in mice measured on the last day of the experiment at autopsy using Vernier calipers and calculated using the formula $V = 4/3\pi r^3$ (n = 11). Columns, mean; bars, SD. (E) Tumor weight was measured at the end of the experiment. Columns, mean; bars, SD.
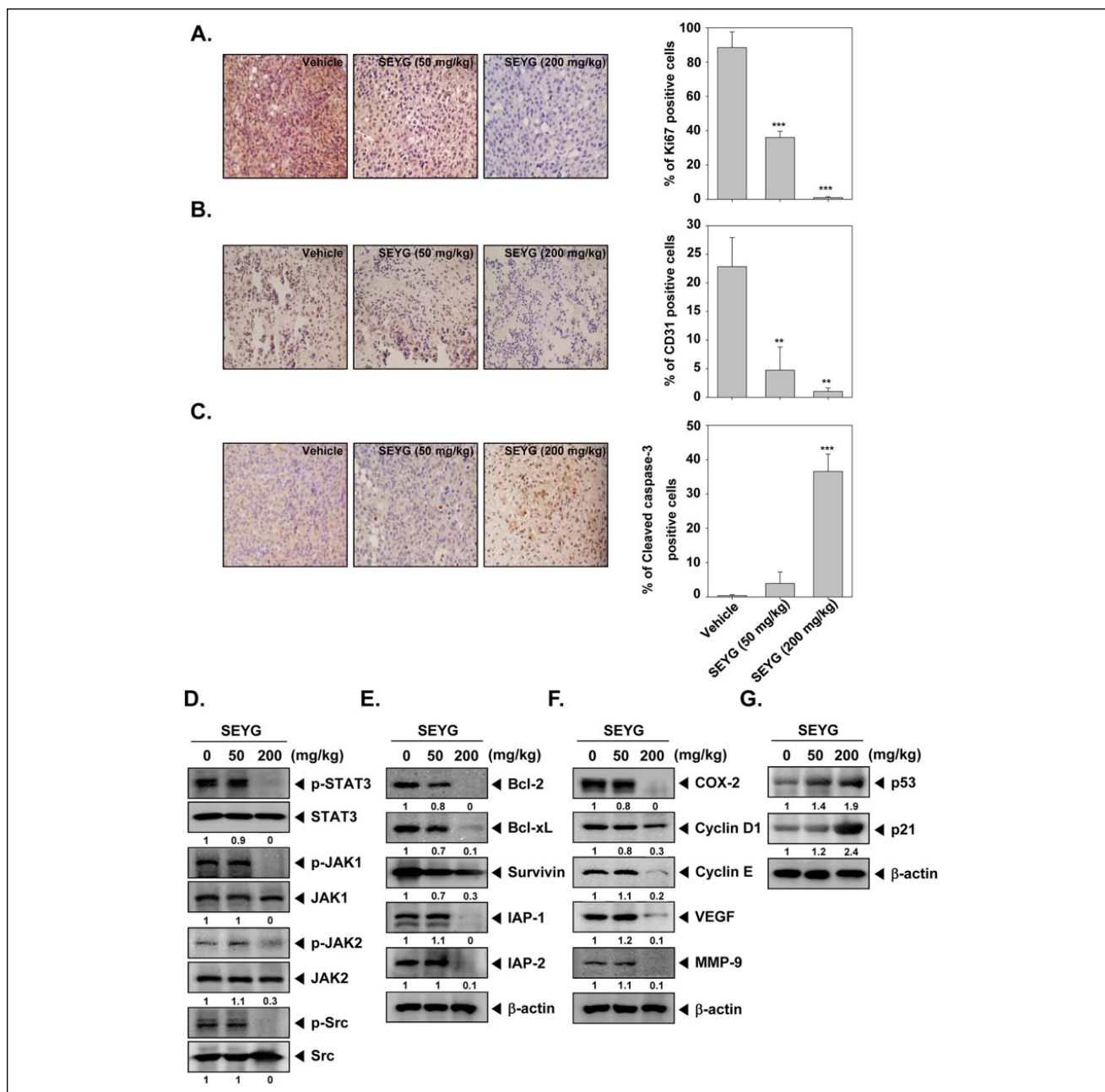
Figure 6. SEYG exerts the effect against tumor cell proliferation and angiogenesis in prostate cancer. (A) Immunohistochemical analysis of proliferation marker Ki-67+ cell indicates the inhibition of human prostate cancer cells proliferation by SEYG dose-dependent treated groups of animals. Samples from 3 animals in each treatment group were analyzed, and representative data are shown (A, *left panel*). Quantification of Ki-67 proliferation index as described in "Materials and Methods." Values are represented as mean ± SD of triplicate (A, *right panel*). Columns, mean of triplicate; bars, SD. (B) Immunohistochemical analysis of CD31 for microvessel density in prostate tumors indicates the inhibition of angiogenesis by SEYG dose-dependent treated groups of animals. Samples from 3 animals in each treatment group were analyzed, and representative data are shown (B, *left panel*). Quantification of CD31 angiogenesis index as described in "Materials and Methods." Values are represented as mean ± SD of triplicate (B, *right panel*). Columns, mean of triplicate; bars, SD. (C) Immunohistochemical analysis of cleaved caspase-3 in prostate tumors. Samples from 3 animals in each treatment group were analyzed, and representative data are shown (C, *left panel*). Quantification of cleaved caspase-3 as described in "Materials and Methods." Values are represented as mean ± SD of triplicate (C, *right panel*). Columns, mean of triplicate; bars, SD. (D) Western blot analysis showed the inhibition of p-STAT3, p-JAK1, p-JAK2, and p-Src by SEYG in whole cell extracts from animal tissue. The same blots were stripped and reprobed with STAT3, JAK1, JAK2, and Src antibody to verify equal protein loading. (E-G) Equal amounts of lysates were analyzed by Western blot analysis using antibodies against bcl-2, bcl-xL, survivin, IAP-1, IAP-2, COX-2, cyclin D1, cyclin E, VEGF, MMP-9, p53, and p21. β-Actin was used as a loading control. Western blotting samples from 3 mice in each group were analyzed and representative data are shown.

prostate tumors from mice by Western blot analysis. Figure 6G shows that SEYG induced the expression of both p53 and p21 gene products in a dose-dependent manner.

Compositional Analysis of SEYG by GC-MS

The extract of yeagam peel was prepared by supercritical extraction method and analyzed by GC/MS. The compounds were identified and listed in Tables 1 and 2. Sixty-four compounds belonging to chemical classes of carboxylic acid (3), alcohol (12), aldehyde (8), ester (10), hydrocarbon (23), ketone (1), and miscellaneous (8) were tentatively identified from the SEYG. Hydrocarbon was the chemical class with the highest proportion, 34.77%. The major hydrocarbon compound was limonene (21.87%). Similarly, esters containing 13.38% were characterized as second major chemical group. Esters of fatty acids were domenent, especially (*Z,Z*)-9,12-octadecanoic acid ethyl ester (8.78%) was detected as a major esterified compound. Monoterpenoidal alcohols, linalool (8.32%) and α-terpineol (2.03%), were major among the alcohol compounds. On the basis of the aforementioned results, it is concluded that limonene was the prime component in SEYG, and major compounds ranged in content order as follows: linalool, geranyl acetate, α-terpineol, β-farnesene, p-cymene, and so on. Next, we quantitatively analyzed the 3 major active compounds in the same extract. The content of limonene, linalool, and geranyl acetate in the extract was 1.21, 0.39, and 0.21 μg/mL, respectively.

Discussion

The purpose of the present study was evaluation of the anticancer activity of SEYG through the blockage of the STAT3 signaling pathway in both in vitro and in vivo. We found that this extract suppressed constitutive STAT3 activation at Tyr705 in human DU145 cells, in parallel with the inhibition of JAK1, JAK2, and c-Src activation. SEYG downregulated the expression of STAT3-regulated gene products, such as bcl-2, bcl-xL, survivin, IAP-1, IAP-2, cyclin D1, COX-2, VEGF, and MMP-9. It also caused the inhibition of proliferation and induced substantial apoptosis in DU145 cells. We further investigated the potential therapeutic efficacy of SEYG in an in vivo model of human prostate carcinoma in mice. Intraperitoneal injection of SEYG in a xenograft mouse model of DU145 cells resulted in a significant suppression of tumor progression, inhibition of STAT3 signaling pathway, and downregulation of various STAT3-regulated gene products in SEYG-treated tumor tissues. Our data clearly indicate that SEYG mediates its suppressive effects on the STAT3 activation cascade in human prostate tumor cells.

This is the first report to evaluate the potential effects of SEYG on STAT3 activation in prostate cancer cells and a xenograft mouse model. Whether examined by STAT3 phosphorylation at tyrosine 705, by nuclear translocation, or by DNA binding, we found that SEYG suppressed STAT3 activation. How SEYG inhibits activation of STAT3 was also investigated in detail. The activation of JAK has been closely linked with STAT3 activation,[20] and we observed that SEYG inhibited the activation of constitutively active JAK1 and JAK2 in DU145 cells. This is in agreement with a report that AZD1480, a specific JAK2 blocker, can suppress the growth of human solid tumors through suppression of STAT3-dependent tumorigenesis.[37]

We further found that SEYG suppressed the expression of several STAT3-regulated genes, including antiapoptotic gene products (bcl-2, bcl-xL, survivin, IAP-1, and IAP-2), proliferative (cyclin D1and cyclin E), angiogenic (COX-2 and VEGF), and metastatic (MMP-9) gene products. The downregulation of cyclin D1and cyclin E expression correlated with suppression in proliferation as observed in DU145 cells. Bcl-2 and bcl-xL can also block cell death induced by a variety of chemotherapeutic drugs, and thus contribute to chemoresistance.[38] In addition, activation of STAT3 signaling can induce *survivin* gene expression and confers resistance to apoptosis in breast cancer cells.[39] Thus, the downregulation of the expression of bcl-2, bcl-xL, and survivin is likely to be linked with SEYG's ability to induce apoptosis in DU145 cells. The downmodulation of VEGF, COX-2, and MMP-9 expression by SEYG also emphasized the antiangiogenic and antimetastatic potential of SEYG in the cells, an aspect that will be investigated in detail in the future.

We also observed that SEYG significantly suppressed human prostate carcinoma growth in a xenograft mouse model as well as downregulated the expression of Ki67 and CD31 and increased the levels of cleaved form of caspase-3 in the treated group as compared with control. Besides, SEYG suppressed STAT3 signaling pathway and a variety of STAT3-regulated gene products from tissues in a xenograft prostate tumor model. Treatment with SEYG (50 mg/kg body weight) did not appear to substantially inhibit the phosphorylation of STAT3, JAK1, JAK2, and Src. However, the volume of tumors in this group is decreased compared with control group. Moreover, to the best of our knowledge, no prior studies with SEYG have been reported in a xenograft prostate tumor model in nude mice, and our observations clearly indicate that SEYG has a clear potential for the treatment of human prostate carcinoma through the suppression of the STAT3 signaling cascade.

Our in vitro and in vivo experimental findings clearly indicate that the anticancer effects of SEYG in human prostate carcinoma are mediated through the suppression of the STAT3 signaling pathway and provide a strong rationale for pursuing the use of SEYG to enhance treatment efficacy in prostate cancer patients.

Table 1. Chemical Compounds Identified From Supercritical Extract of *Citrus iyo* Hort. ex Tanaka Peel.

S. No.	RT	RI	Name	Area % Peel
1	7.72	989	β-Myrcene	0.10
2	7.91	995	(E,E)-2,4-Heptadienal	0.21
3	8.76	1027	**p-Cymene**	**1.30**
4	8.925	1033	**Limonene**	**21.87**
5	9.69	1059	2-Octenal	0.12
6	10.995	1100	**Linalool**	**8.32**
7	12.02	1136	(Z)-Limonene oxide	0.22
8	13.10	1172	Nonanool	0.33
9	13.39	1180	4-Terpineol	0.40
10	13.79	1193	α-**Terpineol**	**2.03**
11	14.145	1204	Decanal	0.26
12	14.27	1209	Octyl acetate	0.22
13	14.64	1222	Carveol	0.18
14	15.56	1255	α-Geraniol	0.18
15	15.80	1264	(E)-2-Decenal	0.02
16	16.295	1279	Perilla aldehyde	0.53
17	16.795	1295	(E,Z)-2,4-Decadienal	0.99
18	16.96	1304	Thymol	0.29
19	17.465	1320	(E,E)-2,4-Decadienal	0.87
20	18.03	1341	δ-Elemene	0.58
21	18.695	1365	Neryl acetate	0.82
22	19.225	1383	**Geranyl acetate**	**2.08**
23	19.575	1395	β-Elemene	0.76
24	19.89	1406	Decyl acetate	0.56
25	20.045	1412	Perillyl acetate	0.48
26	20.415	1428	β-Caryophyllene	0.66
27	20.66	1435	α-Himachalene	0.62
28	20.81	1443	α-Guaiene	0.19
29	21.19	1459	β-**Farnesene**	**1.79**
30	21.325	1462	α-Humulene	0.37
31	22.00	1487	Germacrene-D	0.43
32	22.44	1503	α-Muurolene	0.12
33	22.62	1512	α-Chamigrene	0.24
34	23.07	1530	δ-Cadinene	1.15
35	23.68	1555	Elemol	0.16
36	23.95	1565	(E)-Nerolidol	0.7
37	24.545	1588	Spathulenol	0.66
38	24.7	1594	Caryophyllene oxide	1.42
39	27.26	1702	β-Sinensal	1.63
40	27.835	1729	Isospathulenol	0.58
41	28.59	1763	Tetradecanoic acid	0.76
42	29.905	1822	Nootkatone	1.03
43	30.64	1857	Pentadecanoic acid	0.49
44	31.04	1875	Platambin	0.92
45	33.015	1971	Hexadecanoic acid	2.05
46	33.4	1989	Hexadecanoic acid, ethyl ester	0.38
47	35.36	2093	(Z,Z)-9,12-Octadecanoic acid methyl ester	0.16
48	36.425	2150	(Z,Z)-9,12-Octadecanoic acid ethyl ester	1.2
49	36.63	2160	(Z)-9-Octadecanoic acid ethyl ester	0.48
50	37.28	2194	Docosane	0.33
51	39.085	2295	Tricosane	0.10
52	40.13	2356	2-Methyl tricosane	0.51

Table 1. (continued)

S. No.	RT	RI	Name	Area % Peel
53	40.755	2393	Tetracosane	0.82
54	42.27	2494	Pentacosane	0.16
55	43.25	2568	Hexacosane	0.47
56	44.805	2696	Heptacosane	0.20
57	45.88	2798	Octacosane	0.09
58	46.375	2833	Squalene	1.91
59	50.8	3000<	Tangeritin	3.15
60	51.41	3000<	δ5-Ergostenol	1.03
61	51.845	3000<	Stigmasterol	1.54
62	52.82	3000<	γ-Sitosterol	3.96
63	53.5	3000<	Nobilitin	1.82
64	55.15	3000<	Cycloartenol	0.27
				78.27

Abbreviations: RT, retention time; RI, retention index.

Table 2. Relative Content of Functional Groups of Volatile Organic Compounds Identified in Supercritical Extract of *Citrus iyo* Hort. ex Tanaka Peel.

S. No.	Functional Groups	Relative Peak Area (%)	Number of Compounds
1	Acid (carboxylic)	3.3	3
2	Alcohol	14.75	12
3	Aldehyde	4.63	8
4	Ester	6.38	10
5	Hydrocarbon	34.77	23
6	Ketone	1.03	1
7	Miscellaneous	13.41	8
		78.27	65

Authors' Note

Authors Chulwon Kim and Il Ho Lee contributed equally to this study.

Declaration of Conflicting Interests

The author(s) declared no potential conflicts of interest with respect to the research, authorship, and/or publication of this article.

References

1. Willett WC. Diet and health: what should we eat? *Science*. 1994;264:532-537.

2. Rainer WS. On the history and origin of citrus. *Bull Torrey Bot Club*. 1975;102:369-375.

3. Pienta KJ, Naik H, Akhtar A, et al. Inhibition of spontaneous metastasis in a rat prostate cancer model by oral administration of modified citrus pectin. *J Natl Cancer Inst*. 1995;87:348-353.

4. Hsieh TC, Wu JM. Changes in cell growth, cyclin/kinase, endogenous phosphoproteins and nm23 gene expression in human prostatic JCA-1 cells treated with modified citrus pectin. *Biochem Mol Biol Int*. 1995;37:833-841.

5. So FV, Guthrie N, Chambers AF, Moussa M, Carroll KK. Inhibition of human breast cancer cell proliferation and delay of mammary tumorigenesis by flavonoids and citrus juices. *Nutr Cancer*. 1996;26:167-181.

6. Tanaka T, Kohno H, Tsukio Y, et al. Citrus limonoids obacunone and limonin inhibit azoxymethane-induced colon carcinogenesis in rats. *Biofactors*. 2000;13:213-218.

7. Hayashi A, Gillen AC, Lott JR. Effects of daily oral administration of quercetin chalcone and modified citrus pectin on implanted colon-25 tumor growth in Balb-c mice. *Altern Med Rev*. 2000;5:546-552.

8. Sakata K, Hara A, Hirose Y, et al. Dietary supplementation of the citrus antioxidant auraptene inhibits N,N-diethylnitrosamine-

induced rat hepatocarcinogenesis. *Oncology*. 2004;66: 244-252.

9. Hara A, Sakata K, Yamada Y, et al. Suppression of beta-catenin mutation by dietary exposure of auraptene, a citrus antioxidant, in N,N-diethylnitrosamine-induced hepatocellular carcinomas in rats. *Oncol Rep*. 2005;14:345-351.

10. Luo G, Guan X, Zhou L. Apoptotic effect of citrus fruit extract nobiletin on lung cancer cell line A549 in vitro and in vivo. *Cancer Biol Ther*. 2008;7:966-973.

11. Baek SH, Kim SM, Nam D, et al. Antimetastatic effect of nobiletin through the down-regulation of CXC chemokine receptor type 4 and matrix metallopeptidase-9. *Pharm Biol*. 2012;50:1210-1218.

12. Moon JY, Cho M, Ahn KS, Cho SK. Nobiletin induces apoptosis and potentiates the effects of the anticancer drug 5-fluorouracil in p53-mutated SNU-16 human gastric cancer cells. *Nutr Cancer*. 2013;65:286-295.

13. Dong Y, Cao A, Shi J, et al. Tangeretin, a citrus polymethoxyflavonoid, induces apoptosis of human gastric cancer AGS cells through extrinsic and intrinsic signaling pathways. *Oncol Rep*. 2014;31:1788-1794.

14. Li H, Yang B, Huang J, et al. Naringin inhibits growth potential of human triple-negative breast cancer cells by targeting beta-catenin signaling pathway. *Toxicol Lett*. 2013;220:219-228.

15. Arul D, Subramanian P. Naringenin (citrus flavonone) induces growth inhibition, cell cycle arrest and apoptosis in human hepatocellular carcinoma cells. *Pathol Oncol Res*. 2013;19:763-770.

16. Li F, Chow S, Cheung WH, Chan FL, Chen S, Leung LK. The citrus flavonone hesperetin prevents letrozole-induced bone loss in a mouse model of breast cancer. *J Nutr Biochem*. 2013;24:1112-1116.

17. Darnell JE Jr. STATs and gene regulation. *Science*. 1997;277:1630-1635.

18. Aggarwal BB, Sethi G, Ahn KS, et al. Targeting signal-transducer-and-activator-of-transcription-3 for prevention and therapy of cancer: modern target but ancient solution. *Ann N Y Acad Sci*. 2006;1091:151-169.

19. Chiang SY, Kim SM, Kim C, et al. Antiproliferative effects of Dangyuja (*Citrus grandis* Osbeck) leaves through suppression of constitutive signal transducer and activator of transcription 3 activation in human prostate carcinoma DU145 cells. *J Med Food*. 2012;15:152-160.

20. Ihle JN. STATs: signal transducers and activators of transcription. *Cell*. 1996;84:331-334.

21. Schreiner SJ, Schiavone AP, Smithgall TE. Activation of STAT3 by the Src family kinase Hck requires a functional SH3 domain. *J Biol Chem*. 2002;277:45680-45687.

22. Aggarwal BB, Kunnumakkara AB, Harikumar KB, et al. Signal transducer and activator of transcription-3, inflammation, and cancer: how intimate is the relationship? *Ann N Y Acad Sci*. 2009;1171:59-76.

23. Aggarwal BB, Shishodia S, Sandur SK, Pandey MK, Sethi G. Inflammation and cancer: how hot is the link? *Biochem Pharmacol*. 2006;72:1605-1621.

24. Mosmann T. Rapid colorimetric assay for cellular growth and survival: application to proliferation and cytotoxicity assays. *J Immunol Methods*. 1983;65:55-63.

25. Ahn KS, Sethi G, Sung B, Goel A, Ralhan R, Aggarwal BB. Guggulsterone, a farnesoid X receptor antagonist, inhibits constitutive and inducible STAT3 activation through induction of a protein tyrosine phosphatase SHP-1. *Cancer Res*. 2008;68:4406-4415.

26. Towbin H, Staehelin T, Gordon J. Electrophoretic transfer of proteins from polyacrylamide gels to nitrocellulose sheets: procedure and some applications. *Proc Natl Acad Sci U S A*. 1979;76:4350-4354.

27. Heo JY, Kim HJ, Kim SM, et al. Embelin suppresses STAT3 signaling, proliferation, and survival of multiple myeloma via the protein tyrosine phosphatase PTEN. *Cancer Lett*. 2011;308:71-80.

28. Park KR, Nam D, Yun HM, et al. β-Caryophyllene oxide inhibits growth and induces apoptosis through the suppression of PI3K/AKT/mTOR/S6K1 pathways and ROS-mediated MAPKs activation. *Cancer Lett*. 2011;312:178-188.

29. Kim C, Cho SK, Kim KD, et al. β-Caryophyllene oxide potentiates TNFalpha-induced apoptosis and inhibits invasion through down-modulation of NF-kappa B-regulated gene products. *Apoptosis*. 2014;19:708-718.

30. Adams RP. *Identification of Essential Oils by Ion Trap Mass Spectrometry*. New York, NY: Academic Press; 1989.

31. Bewry NN, Nair RR, Emmons MF, Boulware D, Pinilla-Ibarz J, Hazlehurst LA. Stat3 contributes to resistance toward BCR-ABL inhibitors in a bone marrow microenvironment model of drug resistance. *Mol Cancer Ther*. 2008;7:3169-3175.

32. Deng P, Wang C, Chen L, et al. Sesamin induces cell cycle arrest and apoptosis through the inhibition of signal transducer and activator of transcription 3 signalling in human hepatocellular carcinoma cell line HepG2. *Biol Pharm Bull*. 2013;36:1540-1548.

33. Yu CL, Meyer DJ, Campbell GS, et al. Enhanced DNA-binding activity of a Stat3-related protein in cells transformed by the Src oncoprotein. *Science*. 1995;269:81-83.

34. Kern SE, Kinzler KW, Bruskin A, et al. Identification of p53 as a sequence-specific DNA-binding protein. *Science*. 1991;252:1708-1711.

35. el-Deiry WS, Tokino T, Velculescu VE, et al. WAF1, a potential mediator of p53 tumor suppression. *Cell*. 1993;75: 817-825.

36. Luo Y, Hurwitz J, Massague J. Cell-cycle inhibition by independent CDK and PCNA binding domains in p21Cip1. *Nature*. 1995;375:159-161.

37. Hedvat M, Huszar D, Herrmann A, et al. The JAK2 inhibitor AZD1480 potently blocks Stat3 signaling and oncogenesis in solid tumors. *Cancer Cell*. 2009;16:487-497.

38. Seitz SJ, Schleithoff ES, Koch A, et al. Chemotherapy-induced apoptosis in hepatocellular carcinoma involves the p53 family and is mediated via the extrinsic and the intrinsic pathway. *Int J Cancer*. 2010;126:2049-2066.

39. Gritsko T, Williams A, Turkson J, et al. Persistent activation of stat3 signaling induces survivin gene expression and confers resistance to apoptosis in human breast cancer cells. *Clin Cancer Res*. 2006;12:11-19.